Evidential FastSLAM for Grid Mapping

Thomas Reineking and Joachim Clemens
Cognitive Neuroinformatics
University of Bremen, Germany
{reineking,clemens}@uni-bremen.de

***Abstract*—We present a solution to the problem of simultaneous localization and mapping (SLAM) based on Dempster-Shafer theory. While several works on the mapping problem based on belief functions exist, none of these approaches deal with the full SLAM problem. In this paper, we derive an evidential version of the FastSLAM algorithm based on a Rao-blackwellized particle filter where belief functions are used for representing a grid map of the robot's environment. The resulting algorithm includes the probabilistic FastSLAM solution as a special case without changing its computational complexity. Due to the additional dimensions of uncertainty provided by belief functions, generated maps explicitly show missing information and conflicting sensor measurements. We evaluate our approach using a simulated robot with sonar sensors, for which we derive evidential forward and inverse models. We compare maps obtained by different combination rules and show that the evidential solution outperforms the Bayesian one regarding the resulting localization error.**

I. Introduction

One of the fundamental prerequisites for providing mobile robots with autonomous capabilities is the development of effective solutions to the SLAM problem [1]. During SLAM, the robot has to acquire a map of its environment while localizing itself with respect to that map at the same time, resulting in a joint estimation problem. A particularly successful algorithm for the SLAM problem is FastSLAM [2], which scales well to large environments. This is accomplished via a technique called *Rao-Blackwellization*, by which the joint estimation problem is factored into a path estimation and a conditional mapping problem [3]. The former is solved using a particle filter while the latter can be solved analytically when conditioned on a particular path.

The original FastSLAM algorithm creates a landmark-based representation of the environment in which each landmark is tracked using a separate Kalman filter. A popular alternative to landmark-based representations are occupancy grid maps [4]. Here, the environment is discretized into cells which have a probability of being occupied. Grid maps work particularly well in combination with range sensors like sonar. Another advantage of grid maps is that free space is represented explicitly, making them ideal for navigation. Two applications of FastSLAM to grid mapping are described in [5] and [6].

The occupancy state of each cell in a grid map is usually described by a probability. Dempster-Shafer theory with its belief function formalism constitutes a powerful extension of the classical probability calculus [7]. Belief functions make additional dimensions of uncertainty explicit: missing evidence and conflicting evidence. This is a result of allowing belief mass assignment to arbitrary subsets of a hypothesis space, thereby removing the additivity requirement of probabilities. With belief functions being defined over the power set, a limiting factor for the framework's popularity has been its computational complexity. However, this is not an issue when considering cells that are either occupied or empty, which is why there exist several works where belief functions are used for modeling the occupancy belief in grid maps [8], [9], [10].

All of these works only tackle the mapping aspect of SLAM and ignore the localization part. Our aim in this paper is therefore to develop a Dempster-Shafer-based algorithm for the full SLAM problem that produces 2D grid maps. Our approach resembles the original FastSLAM algorithm and in fact reduces to it in the probabilistic special case. We use a Rao-Blackwellized particle filter for factoring the SLAM problem into a partially probabilistic localization problem and an evidential mapping problem conditioned on the robot's estimated path. As a result, we obtain maps that contain additional information about the underlying uncertainty. On the one hand, belief functions can express ignorance about the occupancy state of a cell by assigning belief mass to the disjunction of *occupied* and *empty*. On the other hand, by using unnormalized belief functions, we gain a representation of the amount of conflict between sensor measurements, both over time and between different sensors.

The paper is structured as follows. In the next section, the equations underlying the evidential FastSLAM approach are derived both for localization and for mapping, and the resulting particle filter algorithm is described. In section 3, evidential forward and inverse models for sonar are presented. In section 4, we show maps generated by different combination rules and compare the corresponding localization error. Finally, in section 5, we discuss some of the key properties of our approach and point out possible extensions.

II. Evidential FastSLAM

The aim during SLAM is to compute the joint distribution over the map Y and the robot's current pose x_t given all sensor measurements $z_{0:t} = z_0, \dots, z_t$ and robot controls $u_{1:t}$.[1] Here, a control u_t describes the change between pose x_{t-1} and x_t. In FastSLAM, one does not only consider the current pose but the entire path $x_{0:t}$. We assume that the marginal distribution over the robot's path can be modeled as a probability density because (i), unlike in the mapping case, there is no practical

[1] We use lower-case letters to denote probabilistic random variables and upper-case letters to denote evidential variables.

reason to explicitly model ignorance and (ii) it would be computationally infeasible (without further restrictions) with poses being continuous. Using this assumption, the joint mass function $m(Y, x_{0:t}|z_{0:t}, u_{1:t})$ over map and path can be factored into a probabilistic localization problem and a conditional, belief-based mapping problem.

$$m(Y, x_{0:t}|z_{0:t}, u_{1:t}) = p(x_{0:t}|z_{0:t}, u_{1:t})\, m(Y|x_{0:t}, z_{0:t}) \quad (1)$$

This factorization is a generalization of the product rule for probabilities.[2] We also exploit the fact that, given the path, the map Y becomes conditionally independent of the control information $u_{1:t}$. In the algorithm described below, the path distribution is approximated using a particle filter whereas the map, conditioned on a specific path, is updated analytically.

A. Localization

Because the robot's pose is modeled probabilistically, the localization is quite similar to classical Markov localization [11]. By applying the generalized Bayesian theorem [12] to $p(x_{0:t}|z_{0:t}, u_{1:t})$, the probability distribution can be factored into the plausibility of the current measurement z_t and a probabilistic prior reflecting all information except for z_t.

$$p(x_{0:t}|z_{0:t}, u_{1:t}) \propto pl(z_t|x_{0:t}, z_{0:t-1})\, p(x_{0:t}|z_{0:t-1}, u_{1:t}) \quad (2)$$

The distribution $p(x_{0:t}|z_{0:t-1}, u_{1:t})$ is referred to as the proposal distribution. Like before, knowing the path makes the controls $u_{1:t}$ conditionally independent of z_t, which is why they are omitted. The crucial part here is $pl(z_t|x_{0:t}, z_{0:t-1})$, which states how likely a measurement is given all previous measurements. Though the distribution over paths is a probability density, the distribution over z_t can be a plausibility (density) function due to the generalized Bayesian theorem. If provided with a map Y and assuming the environment does not change over time, one could exploit conditional independence and the plausibility would reduce to $pl(z_t|x_t, Y)$. Obviously we do not know the true map during SLAM, however, we do have a belief distribution obtained during mapping and thus we can condition the plausibility on the map.

$$pl(z_t|x_{0:t}, z_{0:t-1}) = \sum_{Y \subseteq \Theta_Y^M} pl(z_t|x_t, Y)\, m(Y|x_{0:t-1}, z_{0:t-1}) \quad (3)$$

Here, $pl(z_t|x_t, Y)$ represents the forward sensor model, which we describe in the next section. At first, this equation may appear intractable because of the sum over the power set of the space of all possible maps Θ_Y^M (Θ_Y represents the two-element hypothesis space of a single grid cell and M denotes the total number of cells). However, as shown below, by making an independence assumption between grid cells, the expression can be computed with linear complexity.

The proposal distribution $p(x_{0:t}|z_{0:t-1}, u_{1:t})$ in Eq. (2) can be expressed in terms of a motion model and a prior representing the posterior of the previous time step $t-1$.

$$p(x_{0:t}|z_{0:t-1}, u_{1:t}) = p(x_t|x_{t-1}, u_t)\, p(x_{0:t-1}|z_{0:t-1}, u_{1:t-1}) \quad (4)$$

[2]The proof is quite simple but can not be shown here due to limited space.

By assuming that the robot's path can be modeled as a Markov chain, the motion model only depends on the previous time step. This allows the localization belief to be updated recursively.

B. Grid Mapping

The map belief $m(Y|x_{0:t}, z_{0:t})$ in Eq. (1) is conditioned on the entire path, which is why the individual grid cells can be considered to be approximately independent. This allows us to apply Dempster's rule of combination to split up the joint map belief into M marginal mass functions for each cell Y_i.

$$m_Y(\cdot|x_{0:t}, z_{0:t}) = \bigoplus_{i=1}^{M} m_{Y_i}(\cdot|x_{0:t}, z_{0:t}) \quad (5)$$

This simplification greatly reduces complexity because, in this case, each mass function is only defined over the power set of $\Theta_Y = \{o, \neg o\}$ where o denotes an occupied cell state. Compared to probabilistic grid mapping, this provides two additional parameters for representing uncertainty about a cell: mass on Θ_Y, reflecting ignorance about the cell's state, and mass on $\emptyset$, reflecting the amount of conflict between measurements related to the cell.

Each sensor measurement z_t is assumed to be conditionally independent of all other measurements given the corresponding pose x_t and the map Y. The belief for a single cell Y_i can therefore be updated recursively using, for instance, the (unnormalized) conjunctive rule of combination $\textcircled{\cap}$ (which allows mass on $\emptyset$). However, as we show in section IV, other combination rules can be used as well. Each new measurement z_t induces its own mass function $m(Y_i|x_t, z_t)$, which is combined with the prior belief.

$$m_{Y_i}(\cdot|x_{0:t}, z_{0:t}) = m_{Y_i}(\cdot|x_{1:t-1}, z_{1:t-1}) \,\textcircled{\cap}\, m_{Y_i}(\cdot|x_t, z_t) \quad (6)$$

The belief $m(Y_i|x_t, z_t)$ denotes the inverse sensor model (see next section) and it provides a local map given a single measurement.

C. Algorithm

The basic idea underlying the original FastSLAM algorithm is to use a particle filter for maintaining a set of particles over time, each representing an entire sequence of poses along with a corresponding map of the environment. In our case, the map Y is described by a belief function $m(Y|x_{0:t}, z_{0:t})$, expressing the occupancy state of each grid cell. The particle set $\mathcal{P}_t$ at time t consists of N tuples $(x_{0:t}^{(k)}, Y_t^{(k)})$ with $1 \leq k \leq N$ where $Y_t^{(k)}$ represents the map belief.

Our evidential version of the FastSLAM algorithm is very similar to the original algorithm, with the exception that the forward model returns a plausibility and the map is updated by means of a combination rule (e.g., by the conjunctive rule of combination). New measurements z_t are incorporated into the particle set via importance weighting and a subsequent resampling step [13]. The particle set $\mathcal{P}_t$ at time t is computed recursively from the set $\mathcal{P}_{t-1}$ in the following way:

1) Sample from the motion model $x_t^{(k)} \sim p(x_t|x_{t-1}^{(k)}, u_t)$ in order to incorporate control u_t. The resulting samples

$x_{0:t}^{(k)}$ along with the corresponding maps $Y_{t-1}^{(k)}$ make up the temporary particle set $\overline{\mathcal{P}}_t$ representing the proposal distribution.

2) Compute an importance weight $w_t^{(k)} = pl(z_t|x_{0:t}, z_{0:t-1})$ for each particle in $\overline{\mathcal{P}}_t$ using the map belief $Y_{t-1}^{(k)}$ (see next section). These weights are added to the corresponding particles in $\overline{\mathcal{P}}_t$.
3) Update the map belief $Y_t^{(k)}$ using the inverse model $m(Y|x_t^{(k)}, z_t)$ and an appropriate combination rule.
4) Re-sample particles from $\overline{\mathcal{P}}_t$ with probability proportional to the importance weights. This results in the final (unweighted) particle set $\mathcal{P}_t$ representing the joint path/map belief reflecting all collected evidence.

Though each particle represents an entire path, one can see that only the previous pose is actually used. If not interested in the entire path, one can simply remove all previous poses from a particle, thus keeping the particle size constant over time. In case the importance weights and the map update can be computed efficiently, the algorithm is generally fast enough to be run in real-time. This is because using belief functions only causes a constant performance overhead compared to probabilistic FastSLAM.

III. Forward and Inverse Sensor Model

During both localization and mapping, the robot requires models relating sensor measurements to its pose (localization) as well as to the map (mapping). The former is based on the forward sensor model while the latter is based on the inverse sensor model. These models obviously depend on the specific sensor and, throughout this paper, we focus on sonar. We choose sonar sensors because they provide range measurements about the environment that can be naturally translated into a grid map and because they are subject to significant amounts of uncertainty, making them particularly interesting for an evidential approach. However, the evidential FastSLAM algorithm presented in this paper is not tied to a specific type of sensor and one could just as well devise evidential models for other kinds of sensors. We first define the forward sensor model, both for the case where the map is known and for the case where it is described by a belief function. It turns out that the inverse model can be directly derived from the forward model. Note that readers may safely skip the mathematical derivations presented in this section because they are not essential to understanding the general ideas.

A. Forward Model

The forward model $pl(z_t|x_t, Y)$ specifies the plausibility of a measurement z_t given the current pose x_t and a map $Y \subseteq \Theta_Y^M$. Sonar sensors sometimes produce entirely random range measurements. Let $R \subseteq \Theta_R = \{r, \neg r\}$ denote whether a measurement is random and let $0 \leq \epsilon_r < 1$ denote the maximum chance of receiving a random measurement. We then have the simple support function $m(\neg r) = 1 - \epsilon_r$, $m(\Theta_R) = \epsilon_r$. We set $pl(z_t|x_t, Y, r) = 1$ for any z_t, thereby expressing that any measurement is equally likely in the random case $R = \{r\}$. Using the disjunctive rule of combination [12], we can easily compute $pl(z_t|x_t, Y, \Theta_R)$:

$$pl(z_t|x_t, Y, \Theta_R) = 1 - \prod_{R \in \Theta_R} (1 - pl(z_t|x_t, Y, R)) = 1. \quad (7)$$

This plausibility is 1 for any z_t because it includes the random case. By conditioning the forward model on R, we obtain:

$$pl(z_t|x_t, Y) = \sum_{R \subseteq \Theta_R} pl(z_t|x_t, Y, R)\, m(R) \quad (8)$$

$$= (1 - \epsilon_r)\, pl(z_t|x_t, Y, \neg r) + \epsilon_r. \quad (9)$$

This equation simply states that any measurement has a plausibility of at least ϵ_r. Note that for $z_t \in \mathbb{R}$, one could not define an equivalent probabilistic model without an upper bound for z_t because this would require defining a uniform distribution on $\mathbb{R}$, which is not possible.

For the non-random case, we first define $\widehat{Y}_{1:\widehat{M}}$ as the sequence of cells located in the measurement cone sorted in ascending order by their distance from the current pose. Here, $\widehat{M}$ denotes the number of cells inside of the measurement cone (by definition, cells outside of the measurement cone can not influence the measurement). For notational convenience, we omit x_t and $\neg r$ by setting $pl(z_t|\widehat{Y}_{1:\widehat{M}}) := pl(z_t|x_t, Y, \neg r)$ (the state is indirectly represented by the sequence $\widehat{Y}_{1:\widehat{M}}$ anyway due to the ordering by distance). Furthermore, we write o_k as a shorthand for denoting that the k-th cell is occupied.

We make the simplifying assumption that a sonar sensor always measures the closest occupied cell. Because range measurements are subject to noise, we model their distributions as Gaussians. If the k-th cell causes a measurement, ignoring all other cells, we have a Gaussian measurement likelihood located at the k-th cell with some variance σ_z^2. In contrast, if all cells are empty, a sensor is assumed to return a maximum range value $z_{\max}$.

$$pl(z_t|o_k) = \alpha \mathcal{N}(z_t; \mu_k, \sigma_z^2) \quad (10)$$

$$pl(z_t|\widehat{Y}_{1:\widehat{M}} = \{\neg o\}) = 1_{z_t = z_{\max}} \quad (11)$$

The normalization constant α is necessary to assert that the likelihood is bounded by 1 because it is treated as a plausibility. The indicator function $1_{z_t = z_{\max}}$ returns a likelihood of 1 for the max range value $z_{\max}$ and 0 for all other values.

The constraint of always measuring the closest occupied cell allows us to state two independence properties. First, any cell after the first occupied cell is irrelevant. Second, any empty cell in front of the first occupied cell is irrelevant.

$$pl(z_t|\widehat{Y}_{1:\widehat{M}}) = pl(z_t|\widehat{Y}_{1:k}) \qquad \text{if } \widehat{Y}_k = \{o\} \quad (12)$$

$$pl(z_t|\widehat{Y}_{k:\widehat{M}}) = pl(z_t|\widehat{Y}_{k+1:\widehat{M}}) \qquad \text{if } \widehat{Y}_k = \{\neg o\} \quad (13)$$

By exploiting these independence properties, the forward model can be computed by recursively applying the disjunctive

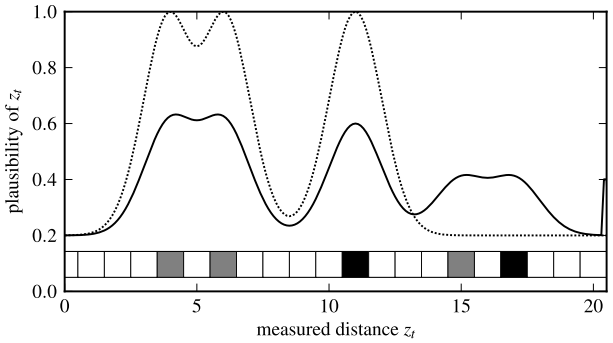

Fig. 1. Forward sensor model as a function of z_t for a one-dimensional map. The dotted line shows the plausibility $pl(z_t|x_t, Y)$ for a given map Y without uncertainty while the continuous line shows the plausibility $pl(z_t|x_{0:t}, z_{0:t-1})$ for the uncertain map case. The squares at the bottom represent the "map": white means $\{\neg o\}$, black means $\{o\}$, and gray means Θ_Y. For the uncertain map case, half of the mass of each black and gray cell is assigned to $\{\neg o\}$ and the remaining mass is assigned to $\{o\}$ (for black cells) or Θ_Y (for gray cells).

rule of combination to the likelihood $pl(z_t|\widehat{Y}_{1:\widehat{M}})$.

$$pl(z_t|\widehat{Y}_{k:\widehat{M}}) = 1 - \prod_{\widehat{y}_k \in \widehat{Y}_k} (1 - pl(z_t|\widehat{y}_k, \widehat{Y}_{k+1:\widehat{M}})) \quad (14)$$

$$= \begin{cases} pl(z_t|o_k) & \text{if } \widehat{Y}_k = \{o\} \\ pl(z_t|\widehat{Y}_{k+1:\widehat{M}}) & \text{if } \widehat{Y}_k = \{\neg o\} \\ pl(z_t|\widehat{Y}_{k+1:\widehat{M}})(1 - pl(z_t|o_k)) & \text{if } \widehat{Y}_k = \Theta_Y \\ \quad + pl(z_t|o_k) & \end{cases}$$

The recursion ends at the first strictly occupied cell due to independence property (12), in which case a likelihood according to (10) is returned. Empty cells are ignored because of independence property (13) while the Θ_Y case is a disjunction of the occupied and empty cases. If there are no strictly occupied cells, the recursion ends at $k = \widehat{M}$ with the max range case defined by Eq. (11).

In the case of localization, the forward model must be conditioned on the map as shown in Eq. (3) because the map generally contains uncertainty. Though the mass functions describing the map can be unnormalized (depending on the combination rule), for localization, we always normalize them in advance. This is because we only allow mass on the empty set for representing conflict in the map and not because we make an open world assumption regarding cells [14]. This is why the case $\widehat{Y}_k = \emptyset$ is omitted in Eq. (14). To simplify notation, we set $m(\widehat{Y}_i) := m(\widehat{Y}_i|x_{1:t-1}, z_{1:t-1})$ and first ignore the possibility of entirely random measurements. We define the conditioning of the forward model with the map starting at cell k (the map belief can be factored due to cell independence) as:

$$S_k := \sum_{\widehat{Y}_k \subseteq \Theta_Y} m(\widehat{Y}_k) \cdots \sum_{\widehat{Y}_{\widehat{M}} \subseteq \Theta_Y} m(\widehat{Y}_{\widehat{M}})\, pl(z_t|\widehat{Y}_{k:\widehat{M}}). \quad (15)$$

Using the same independence properties as before, we can recursively compute the likelihood of a new measurement when all we have is a belief distribution over possible maps.

$$S_k = \sum_{\widehat{Y}_k \subseteq \Theta_Y} m(\widehat{Y}_k) \cdot \begin{cases} pl(z_t|o_k) & \text{if } \widehat{Y}_k = \{o\} \\ S_{k+1} & \text{if } \widehat{Y}_k = \{\neg o\} \\ S_{k+1}(1 - pl(z_t|o_k)) & \text{if } \widehat{Y}_k = \Theta_Y \\ \quad + pl(z_t|o_k) & \end{cases}$$

$$= S_{k+1}(pl(\widehat{Y}_k = \{\neg o\}) - m(\widehat{Y}_k = \Theta_Y)\, pl(z_t|o_k)) + pl(\widehat{Y}_k = \{o\})\, pl(z_t|o_k) \quad (16)$$

Apart from the fact that the different cases have to be weighted by the corresponding map belief and subsequently summed over, this expression is identical to Eq. (14). It can thus be recursively computed in the same fashion (the recursion terminates with $S_{\widehat{M}+1} = 1_{z_t = z_{\max}}$). By also accounting for random measurements (described by the parameter ϵ_r), the final measurement likelihood $pl(z_t|x_{1:t}, z_{1:t-1})$ for the uncertain map case is obtained by:

$$pl(z_t|x_{1:t}, z_{1:t-1}) = (1 - \epsilon_r)\, S_1 + \epsilon_r. \quad (17)$$

Fig. 1 shows the forward model for a map without uncertainty and for one with uncertainty. In the former case, the Θ_Y cells cause high likelihoods for z_t, but because these cells represent the disjunction of *empty* and *occupied*, the likelihoods for non-empty cells at greater distances do not decrease. This only happens after the first occupied cell at $z_t = 11$. In contrast, for the uncertain map case, we assume half the mass of each cell is assigned to *empty*, allowing for the possibility of cells behind a partially occupied cell to be the cause of a measurement. Therefore, the plausibilities do not drop off entirely after the first occupied cell. Both plausibility functions are bounded below by $\epsilon_r = 0.2$ because any z_t has at least this much plausibility due to random measurements. The peak at the very right of the uncertain map case is caused by reaching $z_{\max}$.

B. Inverse Model

The inverse sensor model $m(Y_i|x_t, z_t)$ provides a belief distribution for each cell in the measurement cone (outside we simply set $m(\Theta_Y|x_t, z_t) = 1$). While several belief-based inverse models have been proposed in the literature [8], [9], we obtain our model in a more principled manner by deriving it from the forward model.

As in the case of the forward model, we only consider cells within the measurement cone and we sort cells by their distance (and as a consequence, omit the pose). Unfortunately, it is not possible to directly construct the inverse model by applying the generalized Bayesian theorem to the forward model because the forward model requires the entire map and, in the case of the inverse model, we are only considering a single cell.

This is why we introduce a cause variable $C \subseteq \Theta_C, C \neq \emptyset$ representing the possible causes for a measurement z_t (we assume there is exactly one cause). Either a measurement z_t is caused by an occupied cell k in the measurement cone (denoted by c_k) or, if no cells are occupied, the sensor returns

$z_{\max}$ (denoted by $c_{\widehat{M}+1}$). In addition to these causes, we have to account for the fact that a measurement can be entirely random, which, like in the forward model, is represented by a variable R. We can then condition the inverse model on both C and R:

$$m(\widehat{Y}_i|z_t) = \sum_{R\subseteq\Theta_R} m(R) \sum_{C\subseteq\Theta_c} m(C|z_t)\, m(\widehat{Y}_i|C,R). \quad (18)$$

The distribution of $\widehat{Y}_i$ is conditionally independent of measurement z_t if both C and R are known. In addition, the question whether z_t is random is independent of z_t itself, therefore it is also omitted in $m(R)$. Finally, the distribution of causes C is by definition independent of R.

The mass function $m(\widehat{Y}_i|C,R)$ simply expresses the constraint of always measuring the first occupied cell in the non-random case.

$$m(\widehat{Y}_i = \widehat{y}_i|C,R) = 1 \quad (19)$$

$$\widehat{y}_i = \begin{cases} \{o\} & \text{if } R=\{\neg r\} \wedge C=\{c_i\} \\ \{\neg o\} & \text{if } R=\{\neg r\} \wedge C\subseteq C_{k>i} \\ \Theta_Y & \text{else} \end{cases} \quad (20)$$

$$C_{k>i} := \{c_k | k>i\} \quad (21)$$

If c_i is the measurement cause (and the measurement is not random), the i-th cell must be occupied. Any additional cause (e.g., $C=\{c_i,c_j\}$, $j\neq i$) would, via the disjunctive rule of combination, result in $\widehat{Y}_i = \Theta_Y$. For the case $\widehat{Y}_i = \{\neg o\}$, only subsets from $C_{k>i}$ constitute possible causes (some cell k with $k>i$ caused the measurement), implying that cell i is empty. In all remaining cases, the state of cell i can not be determined and all mass is consequently assigned to Θ_Y.

With this definition of $m(\widehat{Y}_i|C,R)$ and the definition of $m(R=\{\neg r\}) = 1-\epsilon_r$ from the forward model, the masses on *occupied* and *empty* can be computed in the following way (the mass on Θ_Y simply results from normalization):

$$m(\widehat{Y}_i=\{o\}|z_t) = (1-\epsilon_r)\, m(C=\{c_i\}|z_t) \quad (22)$$

$$\begin{aligned} m(\widehat{Y}_i=\{\neg o\}|z_t) &= (1-\epsilon_r) \sum_{C\subseteq C_{k>i}} m(C|z_t) \\ &= (1-\epsilon_r)\, bel(C=C_{k>i}|z_t) \end{aligned} \quad (23)$$

The distribution $m(C|z_t)$ is obtained by applying the generalized Bayesian theorem to the forward model. However, we only consider the map belief marginalized to single cells and different cells can have the same distance with respect to the robot. In this case, mass would only be assigned to the disjunction of the corresponding causes by the generalized Bayesian theorem (see Eq. (24)). If we would consider the joint distribution over cells, this assignment would be fine (and in fact desirable). But because we can only handle the marginal belief over single cells, we need a mechanism ensuring that, even for equidistant cells, the belief for cause c_i can become greater than 0. This is why we introduce a prior m_0 on Θ_C assigning at least some mass π_c strictly to the current cell as a measurement cause while the rest is assigned to Θ_C:

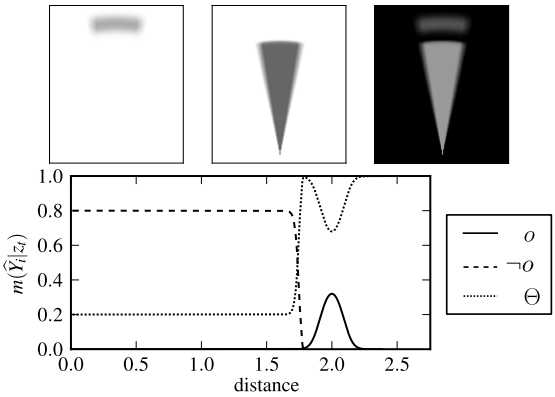

Fig. 2. Inverse sensor model for a measurement of $z_t = 2$. The upper part shows the resulting 2D belief distribution over cells ($m(o)$, $m(\neg o)$, and $m(\Theta_Y)$ from left to right) where darker colors indicate higher values. In the lower part, one can see a one-dimensional projection of the belief distribution as a function of the distance from the robot.

$m_0(C=\{c_i\}) = \pi_c$ and $m_0(C=\Theta_C) = 1-\pi_c$. Higher values of π_c effectively cause higher mass values on $\{o\}$.

Let m' denote the mass function over C *without* the prior m_0 (bel'/pl' are the corresponding belief/plausibility functions). This belief without any prior is computed using the generalized Bayesian theorem [15].

$$m'(C|z_t) = \eta' \prod_{c\in C} pl(z_t|c) \prod_{c\in\overline{C}} (1-pl(z_t|c)) \quad (24)$$

$$bel'(C|z_t) = \eta' \prod_{c\in\overline{C}} (1-pl(z_t|c)) - \eta' \prod_{c\in\Theta_C} (1-pl(z_t|c)) \quad (25)$$

$$pl'(C|z_t) = \eta' \left(1 - \prod_{c\in C} (1-pl(z_t|c))\right) \quad (26)$$

$$\eta'^{-1} = 1 - \prod_{c\in\Theta_C} (1-pl(z_t|c))$$

The belief values required for the inverse model ($m(c_i|z_t)$ and $bel(C_{k>i}|z_t)$) are then computed by combining m' with the prior m_0.

$$m_C(\cdot|z_t) = m_0 \oplus m'_C(\cdot|z_t) \quad (27)$$

$$m(c_i|z_t) = \eta\, (\pi_c\, pl'(c_i|z_t) + (1-\pi_c)\, m'(c_i|z_t)) \quad (28)$$

$$bel(C_{k>i}|z_t) = \eta\, (1-\pi_c)\, bel'(C_{k>i}|z_t) \quad (29)$$

$$\eta^{-1} = 1 - m_0(c_i|z_t)\, (1-pl'(c_i|z_t))$$

Here, η denotes the normalization constant resulting from applying Dempster's rule of combination in Eq. (27). Though computing the generalized Bayesian theorem for each cell appears to be expensive, the complexity of computing the entire inverse model is in fact only $O(\widehat{M})$ if recurring products are saved between computations.

An example of the resulting inverse model is shown in Fig. 2. Here, the measurement cone is clearly visible as well as the arc located at the measured distance where $m(\{o\}) > 0$. As one would expect, the area inside the measurement cone in front of the arc is empty with high belief while the model remains entirely agnostic about the area behind the arc. There is a peak for Θ_Y right in front of the measured distance,

which indicates the high ignorance in this area resulting from measurement noise. Also visible are the "fuzzy" borders at the sides. This is a result of discounting (not shown in the equations), which we use to allow for a smoother transition between cells located inside the measurement cone and cells located outside. Like in the forward model, the parameter ϵ_r forms a lower bound for the mass assigned to Θ_Y.

IV. Experimental Results

In order to evaluate our approach, we use a simulated mobile robot equipped with 8 sonar sensors. Sonar and odometry measurements were recorded for a specified path and, in order to maintain comparability, the same data is used for all our tests. We compare different combination rules for incorporating new measurements into the map according to Eq. (6). In particular, we use the conjunctive rule of combination, Dempster's rule, Yager's rule [16], the cautious rule [17], and Bayesian updating. Throughout all tests, we use 300 particles.

Fig. 3 shows a map resulting from each combination rule. The depicted maps are the ones with the highest cumulative importance weights, i.e., the ones that best fit all measurements. For each map, the mass on $\{o\}$, $\{\neg o\}$, Θ_Y, and $\emptyset$ is shown if the information is available. Regardless of the combination rule, the evidential FastSLAM algorithm is able to capture the essential layout of the environment and manages to successfully close the loop when the robot returns to its initial position.

Among the combination rules considered here, the conjunctive rule is the only one yielding mass on $\emptyset$ and is therefore the only rule allowing for a representation of conflicting evidence. As seen, there is significant conflict in the vicinity of obstacles due to both measurement noise and in some cases localization errors. In general, the conflict is a good indicator for areas that are potentially unsafe because at least some measurements contradict each other regarding the existence of an obstacle. In contrast, the high mass values assigned to Θ_Y in areas the robot did not observe makes the lack of information explicit. Dempster's rule is identical to the conjunctive rule apart from normalization, which is why there is no conflict representation for Dempster's rule. The resulting map is therefore practically identical and is only shown for completeness.

In Yager's rule, all mass that would be assigned to the empty set by the conjunctive rule is instead assigned to the universal set Θ_Y. The result is a map with more mass assigned to Θ_Y around obstacles, expressing the undecidedness of the robot about these cells. Additional measurements in these areas by a less noisy sensor would therefore quickly change the belief.

The cautious rule explicitly allows for dependencies between pieces of evidence. Here, it means that the robot remains much more cautious (hence the name) about areas in the map associated with conflicting measurements. Instead of committing to either *empty* or *occupied*, as Dempster's and Yager's rule (to a degree) eventually tend to do after sufficiently many measurements, most mass is assigned to Θ_Y. This can be particularly desirable when combining the resulting map with one obtained by a different, potentially more precise sensor, in which case this "conservative" estimate makes the limited sonar sensor quality explicit.

For comparison, we also show a map generated using Bayesian updating. In order to maintain comparability between the different approaches, we use the same forward and inverse models and only initialize the map with a uniform Bayesian prior. By using Dempster's rule, the approach then reduces to a probabilistic grid mapping one. In the resulting map, some of the structures visible in the other maps are missing. While this could be due to suboptimal parameters, there is no indication of a possible problem in these areas (like in the other maps with mass assigned to $\emptyset$ or Θ_Y), with almost all probabilities expressing very high certainty.

In order to evaluate the performance of the different rules, we compare their localization error. Fig. 4 shows the localization error corresponding to the particles with the highest cumulative importance weights. As seen, all rules exhibit an increasing localization error until the robot approaches its initial position, where the error decreases again. The evidential rules consistently outperform the Bayesian update rule, in particular the conjunctive rule has a significantly lower localization error.

V. Discussion

In this paper, we have developed an evidential version of the FastSLAM algorithm for grid mapping. The joint belief over the robot's path and the map is assumed to be a hybrid distribution composed of a probability density over paths and a set of belief functions describing the occupancy state of grid cells. Based on this assumption, the joint distribution is factored into its two components and a Rao-Blackwellized particle filter is used for computing the joint belief efficiently. With probabilistic sensor models, our approach would reduce to the probabilistic version of FastSLAM.

Compared to the original FastSLAM algorithm, the evidential algorithm only has a constant computational overhead, which is caused by the additional parameters for each cell. At the same time, these parameters can provide important information, effectively adding two additional dimensions of uncertainty: ignorance about a cell's state and conflict between sensor measurements.[3] A particular advantage of being able to explicitly express ignorance is that it frees one from specifying an occupancy prior, which can be difficult to obtain and is often environment-specific. In contrast, the conflict can be a good measure for "problematic" areas in the map that may require additional measurements in order to reach a higher level of confidence [18]. For navigation, this more nuanced representations of uncertainty could be used for planning safe paths by avoiding conflicting areas. The distinction between conflict and ignorance could also be useful for a robot that tries to actively gather information about its environment. This is because using a probabilistic representation, a near-uniform distribution can mean two fundamentally different

[3]The use of belief functions can also be viewed as a fuzzification of a four-valued logic, consisting of the truth values *true*, *false*, *unknown*, and *contradictory*.

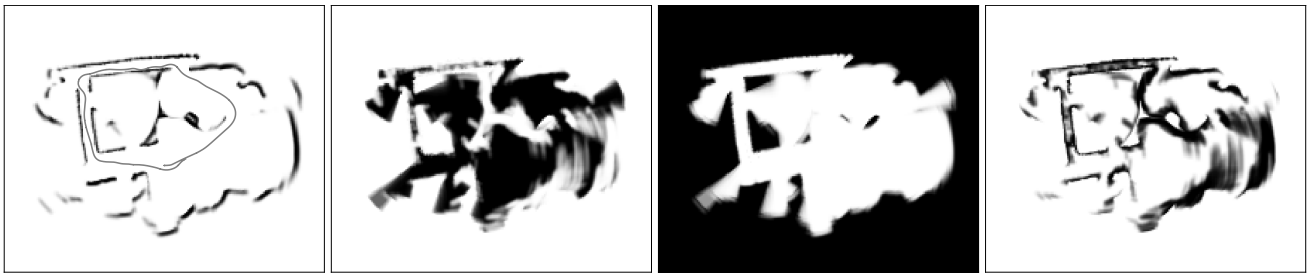

(a) Conjunctive rule

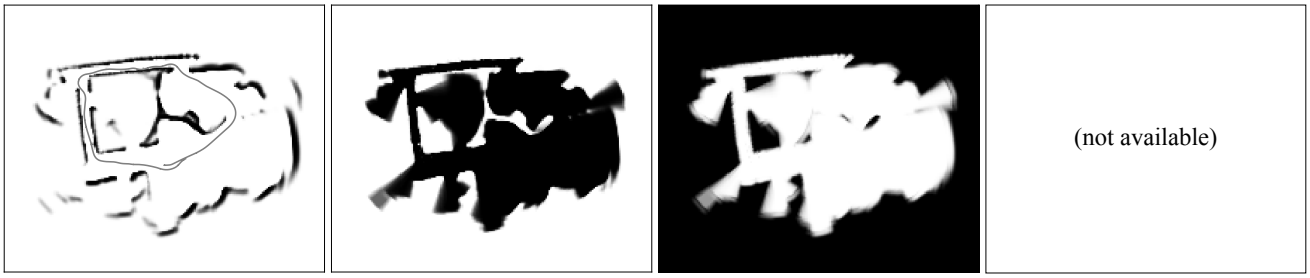

(b) Dempster's rule (no mass on $\emptyset$)

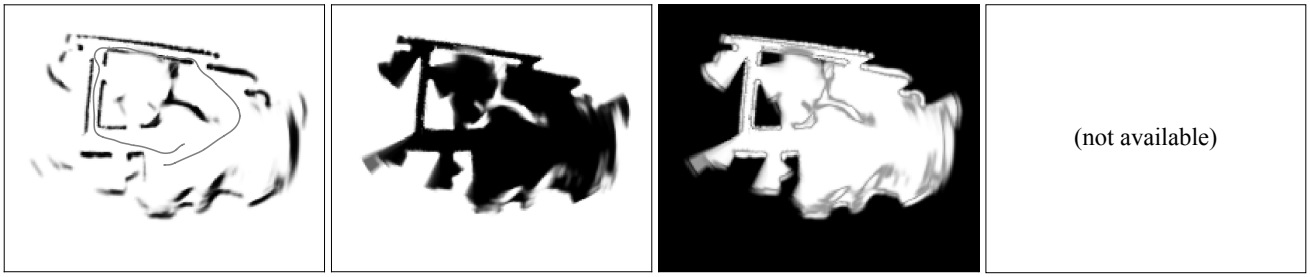

(c) Yager's rule (no mass on $\emptyset$)

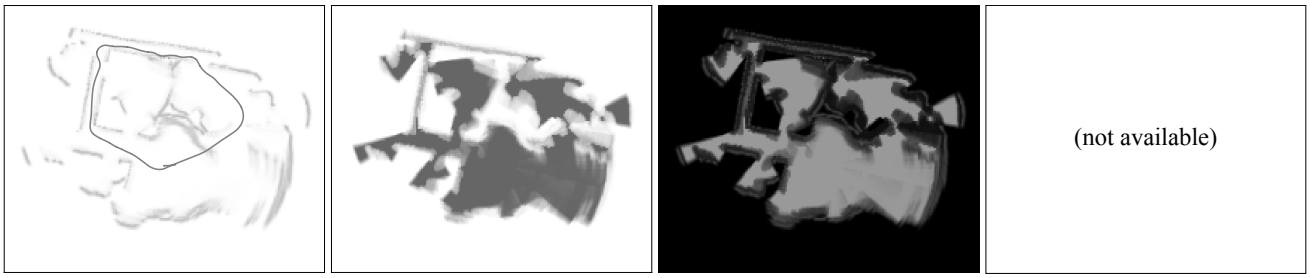

(d) Cautious rule (no mass on $\emptyset$)

(e) Bayesian updating (no mass on $\emptyset$ and Θ_Y)

Fig. 3. Maps generated by different combination rules. Each row of images corresponds to the most likely map generated by a given combination rule. The images within each row represent the different components of a map, in particular (from left to right) the mass on *occupied*, *empty*, Θ_Y, and $\emptyset$. The mass on Θ_Y represents the ignorance while the mass on $\emptyset$ represents the conflict (not all combination rules yield mass on Θ_Y or $\emptyset$). In addition, the estimated path of the simulated robot is shown for each combination rule. Each run was performed using 300 particles and we only show the map with the highest cumulative importance weight.

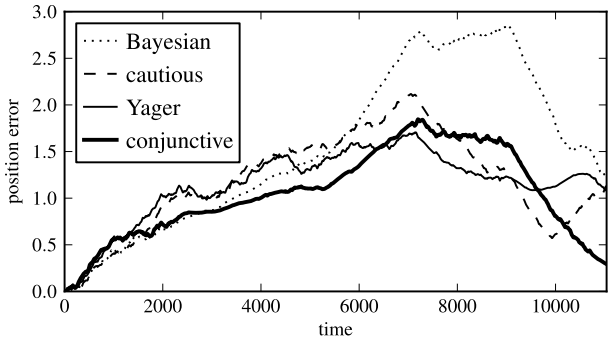

Fig. 4. Distance from the robot's true position over time for different combination rules. For all rules, the error tends to grow over time until the robot approaches its starting position. Overall, the evidential rules result in a smaller localization error compared to the Bayesian solution with the conjunctive rule/Dempster's rule (these are equivalent regarding localization) showing the best performance.

things: either there have been no measurements at all or the measurements could be entirely contradictory, in which case simply collecting more measurements might not help.

Though the algorithm presented in this paper was shown to successfully generate maps, there are several points that should be addressed by future research. A weakness of the original FastSLAM algorithm, from which our approach suffers as well, is its strong reliance on the quality of the proposal distribution, which is usually generated based on the robot's controls. This is why the authors of the original algorithm proposed an improved version FastSLAM 2.0 [19], which incorporates the latest measurement into the proposal distribution, thereby improving the proposal distribution. Another practical issue regarding the presented sensor models is the choice of model parameters. A promising alternative would therefore be to learn these models from data, which raises the interesting research question of how belief functions can be learned from data [20]. Furthermore, we plan to evaluate our approach on a non-simulated mobile robot.

One of the major advantages of the evidential approach is the ability to fuse different information sources of varying quality during mapping [21]. While we have only considered sonar sensors as a first step, this ability in fact becomes much more crucial when using different sensor types that provide complementary and partially overlapping information. The probabilistic solution to fusion in this case is usually based on an absolute independence assumption [22]. In contrast, belief functions could explicitly model the ignorance of a sensor about certain parameters of the map while the resulting conflict between different sensors could also be made explicit. Here, Dempster-Shafer theory with its different combination rules provides a powerful framework for fusing maps in an appropriate manner.

ACKNOWLEDGMENT

This work was supported by DFG (SFB/TR 8 Spatial Cognition, project *A5-[ActionSpace]*) and DLR (project *Enceladus Explorer*).

REFERENCES

[1] H. Durrant-Whyte and T. Bailey, "Simultaneous localization and mapping: part i," *IEEE Robotics & Automation Magazine*, vol. 13, no. 2, pp. 99–110, 2006.

[2] M. Montemerlo, S. Thrun, D. Koller, and B. Wegbreit, "FastSLAM: A factored solution to the simultaneous localization and mapping problem," in *Proceedings of the National conference on Artificial Intelligence*, 2002, pp. 593–598.

[3] A. Doucet, N. De Freitas, K. Murphy, and S. Russell, "Rao-Blackwellised particle filtering for dynamic Bayesian networks," in *Proceedings of the Sixteenth conference on Uncertainty in artificial intelligence*, 2000, pp. 176–183.

[4] A. Elfes, "Using occupancy grids for mobile robot perception and navigation," *Computer*, vol. 22, no. 6, pp. 46–57, 1989.

[5] D. Hähnel, W. Burgard, D. Fox, and S. Thrun, "An efficient FastSLAM algorithm for generating maps of large-scale cyclic environments from raw laser range measurements," in *Intelligent Robots and Systems, 2003.(IROS 2003). Proceedings. 2003 IEEE/RSJ International Conference on*, vol. 1. IEEE, 2003, pp. 206–211.

[6] A. Eliazar and R. Parr, "DP-SLAM: Fast, robust simultaneous localization and mapping without predetermined landmarks," in *International Joint Conference on Artificial Intelligence*, vol. 18, 2003, pp. 1135–1142.

[7] G. Shafer, *A Mathematical Theory of Evidence*. Princeton, NJ: Princeton University Press, 1976.

[8] T. Yang and V. Aitken, "Evidential mapping for mobile robots with range sensors," *IEEE Transactions on Instrumentation and Measurement*, vol. 55, no. 4, pp. 1422–1429, 2006.

[9] J. Mullane, M. Adams, and W. Wijesoma, "Evidential versus bayesian estimation for radar map building," in *ICARCV'06. 9th International Conference on Control, Automation, Robotics and Vision*. IEEE, 2006, pp. 1–8.

[10] M. Ribo and A. Pinz, "A comparison of three uncertainty calculi for building sonar-based occupancy grids," *Robotics and Autonomous Systems*, vol. 35, no. 3-4, pp. 201–209, Jun. 2001.

[11] S. Thrun, D. Fox, W. Burgard, and F. Dellaert, "Robust Monte Carlo localization for mobile robots," *Artificial Intelligence*, vol. 128, no. 1-2, pp. 99–141, 2001.

[12] P. Smets, "Belief functions: The disjunctive rule of combination and the generalized Bayesian theorem," *International Journal of Approximate Reasoning*, vol. 9, pp. 1–35, 1993.

[13] T. Reineking, "Particle filtering in the Dempster-Shafer theory," *International Journal of Approximate Reasoning*, vol. 52, no. 8, pp. 1124–1135, Nov. 2011.

[14] P. Smets, "Belief functions," in *Non Standard Logics for Automated Reasoning*, P. Smets, E. H. Mamdani, D. Dubois, and H. Prade, Eds. Academic Press, London, 1988, pp. 253–286.

[15] F. Delmotte and P. Smets, "Target identification based on the transferable belief model interpretation of Dempster-Shafer model," *IEEE Transactions on Systems, Man, and Cybernetics*, vol. 34, pp. 457–471, 2004.

[16] R. R. Yager, "On the Dempster-Shafer framework and new combination rules," *Information Sciences*, vol. 41, no. 2, pp. 93–137, 1987.

[17] T. Denœux, "Conjunctive and disjunctive combination of belief functions induced by nondistinct bodies of evidence," *Artificial Intelligence*, vol. 172, no. 2-3, pp. 234–264, Feb. 2008.

[18] J. Carlson, R. Murphy, S. Christopher, and J. Casper, "Conflict metric as a measure of sensing quality," *Proceedings of the 2005 IEEE International Conference on Robotics and Automation*, pp. 2032–2039, 2005.

[19] M. Montemerlo, S. Thrun, D. Koller, and B. Wegbreit, "FastSLAM 2.0: An improved particle filtering algorithm for simultaneous localization and mapping that provably converges," *International Joint Conference on Artificial Intelligence*, vol. 18, pp. 1151—-1156, 2003.

[20] A. Aregui and T. Denœux, "Constructing consonant belief functions from sample data using confidence sets of pignistic probabilities," *International Journal of Approximate Reasoning*, vol. 49, no. 3, pp. 575–594, Nov. 2008.

[21] M. Kurdej, J. Moras, V. Cherfaoui, and P. Bonnifait, "Map-aided fusion using evidential grids for mobile perception in urban environment," *Proceedings of the 2nd International Conference on Belief Functions*, vol. 164, pp. 343–350, 2012.

[22] S. Thrun, W. Burgard, and D. Fox, *Probabilistic robotics*. MIT press Cambridge, MA, 2005, chapter 9.